Received: 25 October 2022 | Revised: 3 January 2023 | Accepted: 4 January 2023

DOI: 10.1002/jor.25513

RESEARCH ARTICLE

Journal of Orthopaedic Research®

Epigenetic dysregulation of articular cartilage during progression of hip femoroacetabular impingement disease

Tomoyuki Kamenaga | Jie Shen | May Wu | Robert H. Brophy | John C. Clohisy | Regis J. O'Keefe | Cecilia Pascual-Garrido

Department of Orthopaedic Surgery, Washington University School of Medicine, St. Louis, Missouri, USA

Correspondence
Cecilia Pascual-Garrido, Department of Orthopaedic Surgery, Washington University School of Medicine, 660S. Euclid Ave., Campus Box 8233-0004-5505, St. Louis, MO 63110, USA.
Email: cpascualgarrido@wustl.edu

Funding information
Orthopaedic Research and Education Foundation, Grant/Award Numbers: 18-003, 20-058; National Institutes of Health, Grant/Award Numbers: 1K08AR077740-01, R01AR069605

Abstract

Femoroacetabular impingement (FAI) is an important trigger of hip osteoarthritis (OA). Epigenetic changes in DNA methyltransferase 3B (DNMT3B) attenuate catabolic gene expression in cartilage hemostasis. This study aimed to examine the articular chondrocyte catabolic state and DNMT3B and 4-aminobutyrate aminotransferase promoter (ABAT) expression during OA progression in FAI. Cartilage samples were collected from the impingement zone of 12 patients with cam FAI (early-FAI) and 12 patients with advanced OA secondary to cam FAI (late-FAI-OA). Five healthy samples were procured from cadavers (ND: nondiseased). Explants were cultured under unstimulated conditions, catabolic stimulus (IL1β), or anabolic stimulus (TGFβ). Histology was performed with safranin-O/fast-green staining. Gene expression was analyzed via qPCR for *GAPDH*, *DNMT3B*, *ABAT*, *MMP-13*, *COL10A1*. Methylation specific PCR assessed methylation status at the *ABAT* promoter. Cartilage samples in early-FAI and late-FAI-OA showed a histological OA phenotype and increased catabolic marker expression (*MMP13*/*COL10A1*, ND vs. early-FAI, $p = 0.004$/$p < 0.001$, ND vs. late-FAI-OA, $p < 0.001$/$p < 0.001$). RT-PCR confirmed *DNMT3B* underexpression (ND vs. early-FAI, $p < 0.001$, early-FAI vs. late-FAI-OA, $p = 0.016$) and *ABAT* overexpression (ND vs. early-FAI, $p < 0.001$, early vs. late-FAI-OA, $p = 0.035$) with advanced disease. End-stage disease showed *ABAT* promoter hypomethylation. IL1β stimulus accentuated *ABAT* promoter hypomethylation and led to further *ABAT* and catabolic marker overexpression in early-FAI and late-FAI-OA while TGFβ normalized these alterations in gene expression. Catabolic and epigenetic molecule expression suggested less catabolism in early-stage disease. Sustained inflammation induced *ABAT* promoter hypo-methylation causing a catabolic phenotype. Suppression of ABAT by methylation control could be a new target for therapeutic intervention to prevent OA progression in hip FAI.

KEYWORDS
articular cartilage, DNA methylation, epigenetic, femoroacetabular impingement, hip osteoarthritis

1 | INTRODUCTION

Osteoarthritis (OA) is the most frequent joint disease affecting 30 million adults in the United States.[1,2] The OA pathophysiology has been clarified mostly using tissues from end stage disease; however, precipitating molecular changes take place in early disease stages.[3,4] Femoroacetabular impingement (FAI) is well-known important etiologic factor for hip OA,[5,6] and is spotted as a leading trigger of degenerative arthritis in the hip.[6,7] Thus, FAI offers a valuable chance to study early molecular changes in hip OA.

Several studies have elucidated the expression of specific genes in articular cartilage from hips with FAI. Cartilage samples from the impingement zone were found to express highly inflammatory and catabolic markers such as matrix metalloproteinase 13 (MMP13) and a disintegrin and metalloproteinase with thrombospondin motif 4 (ADAMTS4), confirming a catabolic phenotype compared to the nondiseased (ND) cartilage.[8–10] However, these studies could not identify a detectable difference between the early and late stages of disease. Recent transcriptome analysis has characterized a distinct transcriptome profile of early-stage FAI, which differs from late-stage hip OA secondary to FAI.[11] The study also found several key genes and pathways that should be explored as potential therapeutic targets for hip OA.[11] In further exploring therapeutic approaches to slow down OA progression in FAI, the anabolic and catabolic states of articular cartilages (ACs) should be evaluated to test whether the FAI-specific cartilage phenotype can be modulated by some therapeutic interventions.

Recent investigations into OA pathophysiology have shown that OA progression is associated with abnormal epigenetic changes of many OA-susceptible genes, suggesting that the onset and progression of OA is also coordinated by unclarified epigenetic mechanisms.[12] Specifically, DNA methyltransferase 3B (Dnmt3b), one of the DNA methyltransferases, is reported to be highly expressed in healthy murine and human cartilage.[13] Additionally, previous murine studies showed that Dnmt3b loss of function leads to the reduction of DNA methylation at the 4-aminobutyrate aminotransferase promoter (Abat), causing overexpression of this gene and subsequent cartilage damage in the knee joint.[13,14] In murine models, inhibition of Abat has shown to block the development of OA following knee joint injury.[14] These studies suggest that Dnmt3b regulates post-natal articular cartilage homeostasis and that Abat is a downstream target for Dnmt3b, attenuating catabolic gene expression.[13,14] However, there is scant evidence of the role of ABAT in the pathogenesis of human OA, and to the best of our knowledge, there are no studies addressing the expression of DNMT3B and ABAT in the progression of hip OA.

The purposes of the present study are: (1) to examine the catabolic and anabolic states of ACs during FAI progression, (2) to assess the expression levels of DNMT3B, ABAT and DNA methylation status at the ABAT promoter site during early (early-FAI) and late (late-FAI-OA) stage disease, and (3) to assess if an inflammatory stimulus dysregulates DNA methylation at the ABAT promoter site. We hypothesized that (1) ACs in early stage hip FAI present a less catabolic phenotype than late stage disease, (2) human hip ACs show decreased expression of DNMT3B and overexpression of ABAT as OA progresses, and (3) an inflammatory stimulus (interleukin1: IL1β) dysregulates methylation at the ABAT promoter site in FAI, and TGFβ alleviate dysregulation of methylation at this site and rescue ACs from catabolic phenotype.

2 | METHODS

2.1 | Patients

This study was approved by the institutional review board (NO. 202007168). Patients who underwent hip preservation surgery or total hip replacement (THR) were enrolled in a longitudinal prospective cohort. All surgical procedures were performed by two experienced surgeons (C. P-G. and J. C. C.) between April 2021 and November 2021. Patients with prior hip surgery, pincer morphology, infection, idiopathic osteonecrosis of the femoral head, psoriasis, and rheumatoid arthritis, were excluded in this study. Full-thickness cartilage samples from the anterolateral head-neck junction of 24 patients undergoing hip surgery were included. Of these, 12 patients underwent hip surgery for the symptomatic cam FAI (early-FAI; $n = 12$) and 12 patients underwent THR for the advanced OA secondary to cam FAI (late-FAI-OA; $n = 12$).

The diagnosis of cam FAI or OA was determined by the treating surgeons (C. P-G. and J. C. C.) using the minimum basic criteria of pain in the affected hip for a period of more than 3 months, hip range of motion, radiographic findings, and intraoperative findings. The Tönnis classification[15] was used to define the OA severity: Early-FAI was diagnosed in patients with Tönnis grades 0–1 and late-FAI-OA in patients with Tönnis grades 2–3. A cam deformity was defined by an alpha angle greater than 55° on the preoperative anteroposterior (AP) pelvic, frog-leg lateral, and/or 45° on Dunn radiographs.[16] All radiographs were performed with a standardized protocol including a standing AP pelvis, 45° Dunn, and frog-leg lateral view. Interobserver and intraobserver reliability of the radiographic analysis of FAI was previously performed by our group.[17] ND healthy samples (control, $n = 5$) were harvested from the anterolateral head-neck area of fresh femoral head allografts with similar methodology. Femoral head fresh grafts were only used if they had macroscopically normal articular cartilage and the donor's age was less than 30-year-old without any history of hip OA and articular cartilage was macroscopically judged as normal by two hip surgeons (C. P-G. and T. K). Allografts were obtained within 24 h of donor death (JRF Ortho) and delivered to the laboratory in a cell culture medium at 4°C.

2.2 | Cartilage sample collection

Full-thickness cartilage samples were obtained through use of a liberator and an arthroscopic biter in arthroscopic procedures or a half-inch osteotome in patients undergoing either open surgical dislocation or THR. All samples were obtained from the anterolateral aspect of the head-neck junction (impingement area) of the proximal femur. Dynamic impingement area was evaluated intraoperatively and care was taken to harvest

cartilage tissue from the most affected areas (visible chondromalacia and discoloration) localized between the 12- and 3-o'clock positions.

2.3 | Human cartilage explant culture

Obtained cartilage samples were used to perform cartilage explant cultures. These included early-FAI ($n = 12$), late-FAI-OA ($n = 12$), and control ND healthy samples ($n = 5$). The experiment was performed according to methods previously described by Yan et al.[18] All cartilage samples were stored in Hank's balanced salt solution (HBSS) immediately after being harvested and transported within 2 h to the laboratory. Immediately after transporting the tissue to the laboratory, explanted cartilage tissue was washed several times with HBSS containing antibiotics and then incubated in Dulbecco's Modified Eagle Medium/Nutrient Mixture F-12 (DMEM/F12) medium containing 10% Fetal Bovine Serum (FBS), penicillin/streptomycin (100 U/0.1 mg/ml) in a 6-well plate at 37°C and 5% CO2 for 48 h.

Then, explants were cultured either in an untreated condition, under a catabolic stimulus with interleukin1 (IL1β) (1.0 ng/ml, Peprotech),[19,20] or under an anabolic stimulus with transforming growth factor-beta (5.0 ng/ml, TGFβ)[21] for 48 h. Of the 12 samples in the early-FAI and late-FAI-OA groups, 6 were used for histological analysis and immunofluorescence analysis, while the remaining 6 were used for western blots and PCRs. This is because the affected cartilage was limited and insufficient to perform all the experiments with a single sample. In the ND group, one cartilage sample was sufficient to perform all experiments.

(Figure 1 shows cartilage culture and experiments).

2.4 | Histological assessment

Following culture, cartilage explant specimens were fixed in 10% neutral buffered formalin for 24 to 48 h, decalcified in Immunocal (Stat-Lab) for 3 days, dehydrated in graded ethanol, embedded in paraffin wax, and sectioned to a thickness of 5 mm by standard protocol[10] ($n = 6$ for early-FAI and late-FAI-OA, $n = 5$ for ND). Safranin-O/fast green staining was performed to histologically evaluate the cartilage degeneration of five samples in each group. Cartilage degeneration was graded in blinded fashion based on the Mankin score.[22] On this scale (normal = 0), cartilage is graded on structural compromise (0–6 points), loss of matrix staining (0–4), anomalies in cellularity (0–3), and violation of tidemark integrity (0–1), with a total score of 0–14 points (0 as the best and 14 as the worst).[22]

2.5 | Gene expression analysis

Real-time polymerase chain reaction (RT-PCR) was performed to assess the expression levels of genes including: *DNMT3B*, *ABAT*, *MMP13*, *COL10A1*, and *COL2A1* ($n = 6$ for early-FAI and late-FAI-OA groups, $n = 5$ for ND group). Total RNA was extracted from cartilage tissue and reverse-transcribed into cDNA using the High-Capacity cDNA Reverse Transcription Kit (Applied Biosystems). RT-PCR amplification of the cDNA was performed in triplicates using SYBR Green reagent (Applied

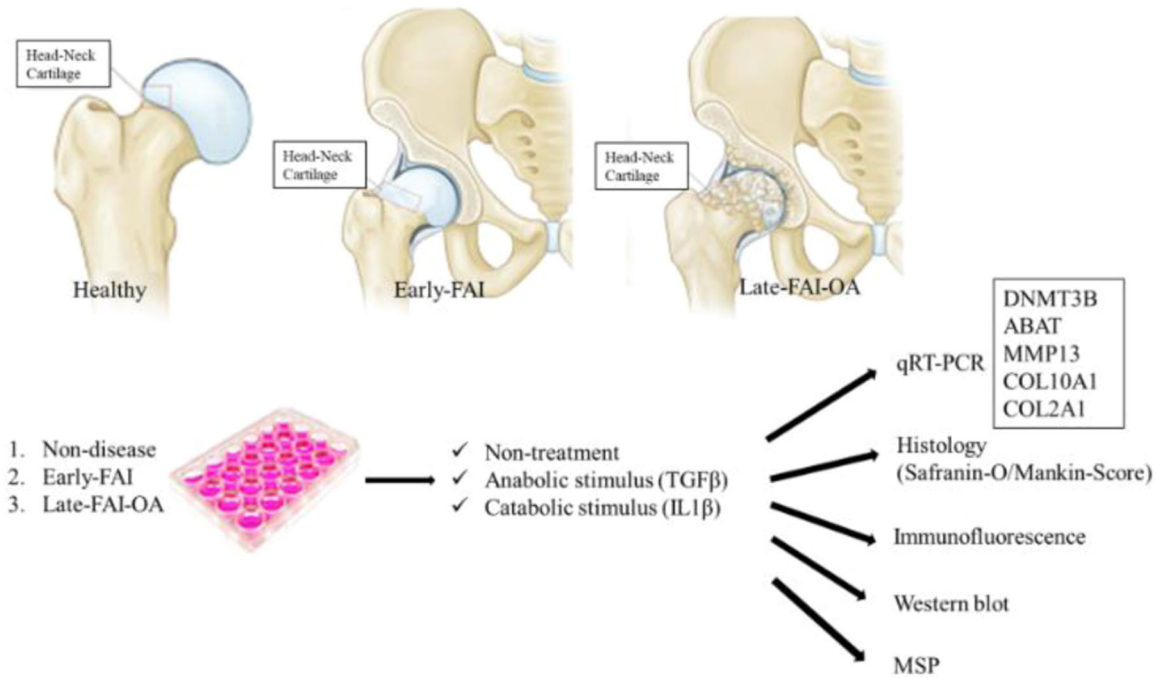

FIGURE 1 Study design. DNMT; DNA methyltransferase; FAI, femoroacetabular impingement; MSP, methylation specific PCR; OA, osteoarthritis; PPARγ; peroxisome proliferator-activated receptor-gamma; RT-PCR, real-time polymerase chain reaction. [Color figure can be viewed at wileyonlinelibrary.com]

TABLE 1 Primer sequences for real-time qPCR

Genes	Sequences (5′-3′)
DNMT3B-F	TTGATATTCCCCTCGTGCTTC
DNMT3B-R	CGAGTCCTGTCATTGTTTGATG
ABAT-F	CAGGTGTTGAAGATCCGGTAG
ABAT-R	CAGCAGACGTGATGACCTTC
MMP13-F	CTTGACCACTCCAAGGACCC
MMP13-R	CCTGGACCATAGAGAGACTGGA
COL2A1-F	ACCAGATTGAGAGCATCCGC
COL2A1-R	AAAACCTTCATGGCGTCCAA
COL10A1-F	CCCTTTTTGCTGCTAGTATCC
COL10A1-R	CTGTTGTCCAGGTTTTCCTGGCAC
GAPDH-F	GACAGTCAGCCGCATCTTCT
GAPDH-R	GCGCCCAATACGACCAAATC

Biosystems). Relative gene expression was normalized against the housekeeping gene glyceraldehyde 3-phosphate dehydrogenase (*GAPDH*) using the comparative cycle threshold method.[23] Relative gene expression was normalized to the mean value of the ND group samples for each gene. Primer sequences were listed in Table 1.

2.6 | Immunofluorescence (IF) analysis

Fluorescent immunostaining was performed as previously described[22] ($n = 6$ for early-FAI and late-FAI-OA, $n = 5$ for ND). After deparaffinization, sections were permeabilized with Sodium Citrate Buffer (10 mM Sodium Citrate, 0.05% Tween-20, pH 6.0) and blocked with 2.5% Donkey serum for 2 h at room temperature. After blocking, the sections were incubated with the primary antibodies, DNMT3B (1:200, Cat# A7239; Abcam) and ABAT (1:200, Cat# sc-393769; Santa Cruz Biotechnology), overnight at 4°C. After washing, the sections were incubated with the corresponding secondary antibody, Goat Anti-Rabbit IgG H&L (Alexa Fluor® 488) (1:200, Cat# ab150077, Abcam), for 2 h. The sections were probed with COL2 antibody (1:200, Cat# sc-518017, Santa Cruz Biotechnology) followed by TRITC-conjugated anti-rat secondary antibody (1:100, Cat# 712-295-153, Jackson ImmunoResearch). Nuclei were counter-stained with DAPI solution (1:1,000, Vector Laboratories) for 5 min. The images were acquired with ZEISS LSM 880 Confocal Laser Scanning Microscope. The data was presented as the mean ratio of positive cells. The number of positive cells was determined as the average cell count in five randomly selected fields in each section under a fluorescent microscope.

2.7 | Western-blot analysis

First, the cultured cartilage samples were washed with Tris-buffered saline with Tween-20 (TBST) and lysed in a lysis buffer. The lysates were centrifuged at 4°C at 15,000 *g* for 10 min. Next, the debris-free lysates were collected and mixed with 4× electrophoresis sample buffer; 30 µg of protein were electrophoresed on a 15% SDS-polyacrylamide gradient gel and electrically transferred onto a polyvinylidene difluoride blotting membrane. The membrane was blocked with 5% bovine serum albumin in TBST at 25°C for 30 min, incubated with primary antibodies against DNMT3B (Cat# A7239, Abcam) and ABAT (Cat# sc-393769, Santa Cruz Biotechnology) at 4°C for 12 h (overnight), and further incubated with horseradish peroxidase-conjugated goat anti-rabbit IgG secondary antibody (Cat# ab216773, Abcam) at 25°C for 1 h. The results were quantified, and the images were processed using ImageJ software (National Institutes of Health). β-actin was used as an internal loading control.

2.8 | Methylation specific PCR (MSP)

According to previous established methods,[24,25] the primer of the *ABAT* promoter for MSP was designed with MetPrimer software (https://www.urogene.org/methprimer).[26] Genomic DNA isolated from ACs was enzymatically digested by methylation-sensitive or methylation-dependent enzymes separately ($n = 5$ for all groups).

The primer sequences were the following: methylated primers (forward/reverse); TTTAGAGATCGGATTCGAGAC/AAACGACTAAAAACCCCCGT, unmethylated primers (forward/reverse); TTAGAGATTGGATTTGAGATG/ACAACTAAAAACCCCCATCA.

2.9 | Statistical analysis

Statistical analyses were performed using GraphPad Prism 9 (GraphPad Software). The comparisons between groups were performed using the Man–Whitney U, one-way analysis of variance (ANOVA), or Kruskal–Wallis tests. Multiple comparisons were performed with the post hoc test with Bonferroni correction if needed. The level of significance was set at $p < 0.05$. Datas are presented as mean ± standard deviation for parametric test and median with range for nonparametric test.

Sample size calculations were performed using G*Power 3 (Heinrich-Heine-Universität Düsseldorf).[27] The minimum sample size required to detect an effect size f of 1.0 in ANOVA was 15 samples (5 samples in each group) when using a type I error (a) of 0.05 and power (1 − b) of 0.80.

3 | RESULTS

3.1 | Characteristics of study patients

Characteristics of study participants are presented in Table 2. The early-FAI group included younger patients. There were no significant differences in gender, BMI, LCEA and α-angle between groups.

TABLE 2 Patient characteristics

Group	Nondisease	Early-FAI	Late-FAI-OA	*p* Value
Number	5	12	12	
Age (years)	27.7 ± 2.4	34.5 ± 10.6	50.7 ± 7.3	<0.001
Gender male/female	3/2	7/5	5/7	0.68
BMI (kg/m^2)	-	28.7 (25.1–35.4)	32.0 (20.7–38.1)	0.59
Radiographs: α angle (degree)	-	67.0 (57.9–87.5)	67.5 (61.0–94.2)	0.42
LCEA (degree)		27.7 (25.5–39.4)	31.6 (25.6–38.2)	0.34

Note: *p* Values (early-FAI vs. late-FAI-OA) are shown.

Abbreviations: BMI, body mass index; FAI, femoroacetabuilar impingement; LCEA, lateral center edge angle; OA, osteoarthritis.

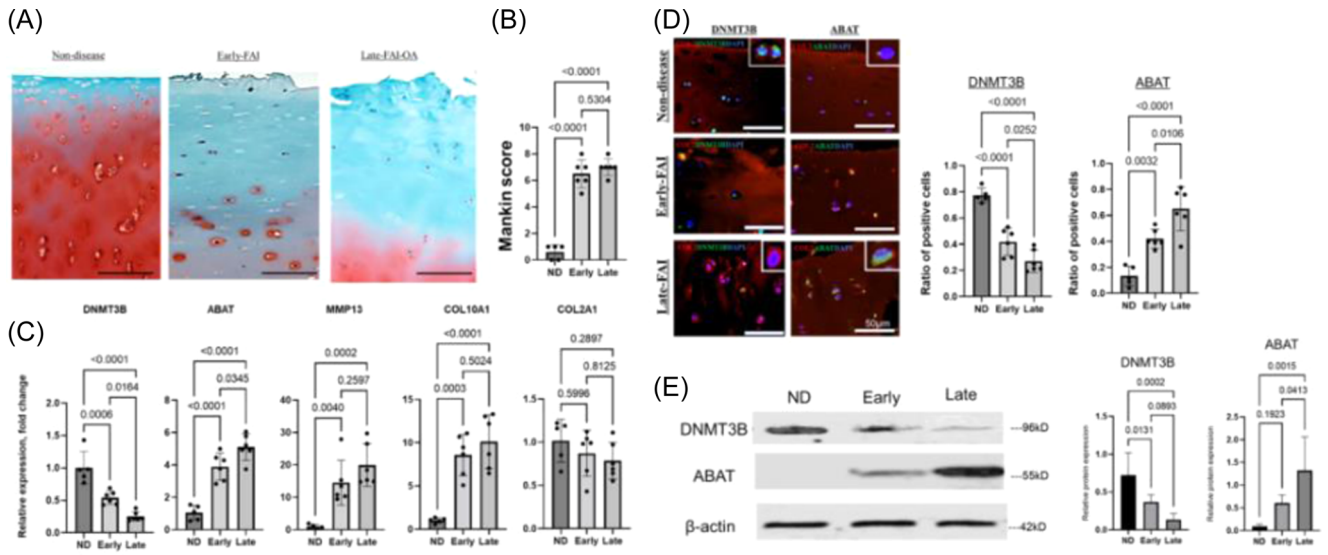

FIGURE 2 Alteration of cartilage phenotype during disease progression. (A) Representative histologic sections of the cartilage stained with safranin-O/fast green. Scale bar: 100 μm. (B) Bar graphs comparing cartilage degeneration using the Mankin score system. (C) Expression of DNMT3B, ABAT, MMP13, COL10A1, and COL2A1 in each group, as determined by RT-PCR. (D) Representative immunofluorescence staining of DNMT3B (green) and ABAT (green) in cartilage sections. COL2 (red), type II collagen; DAPI (blue) stained nuclei. Scale bar: 50 μm. Bar plot showing the quantitative analysis of the ratio of positive cells (DNMT3B and ABAT). (E) Western blot analysis of DNMT3B and ABAT from cartilage samples. β-actin served as the internal control. Graphs show the quantitative analysis. Early, early-FAI; FAI, femoroacetabular impingement; Late, late-FAI-OA; ND, nondisease; OA, osteoarthritis. [Color figure can be viewed at wileyonlinelibrary.com]

3.2 | Cartilage phenotype is altered in progressing hip FAI disease

As a beginning in investigating cartilage phenotype associated with hip OA progression, we performed histological and gene expression analysis for comparison between the disease stages. The ND group samples displayed normal hyaline cartilage, but the early-FAI and late-FAI-OA groups showed degenerative cartilage damage including clefts, cell cloning, and reduced staining of safranin-O (Figure 2A,B, quantified by Mankin Score). Histological findings were similar for early-FAI and late-FAI-OA, and there was no significant difference in Mankin score between the two groups (Figure 2A,B). Using RT-PCR, cartilage in early FAI and late-FAI-OA displayed higher expression of *MMP-13* and *COL10A1* compared to the ND group, confirming the presence of cartilage degeneration, catabolism, and chondrocyte hypertrophy. RT-PCR revealed that expression of *DNMT3B* gradually declined while *ABAT* was impressively increased throughout disease progression (Figure 2C). IF staining confirmed that DNMT3B was abundantly expressed in chondrocytes of normal cartilage but gradually decreased with disease progression; contrarily, ABAT expression gradually increased with disease progression (Figure 2D). Similarly, western blotting displayed decreased DNMT3B protein and increased ABAT protein quantities as the disease progressed (Figure 2E).

3.3 | Catabolic/anabolic stimulus alter the cartilage phenotype in the early and late stages of hip FAI

To investigate the catabolic and anabolic state of articular cartilage during the hip OA progression, cartilage explants were cultured with either no stimulus or vehicle, under catabolic stimulus with IL1β, or under anabolic stimulus with TGFβ for both early-FAI and late-FAI-OA. Histological degenerative changes were more pronounced under IL1β treatment and were alleviated by TGFβ treatment in the early-FAI and late-FAI-OA samples, quantified by the Mankin-score (Figure 3A,B). According to RT-PCR, a catabolic stimulus with IL1β for both early-FAI and late-FAI-OA resulted in overexpression of *ABAT*, *MMP-13*, and *COL10A1* and decreased expression of *DNMT3B*, although abnormal expression of these molecules were effectively normalized with TGFβ treatment (Figure 3B). Furthermore, IF analysis displayed decreased expression of DNMT3B and increased expression of ABAT when treated with IL1β, while treatment with TGFβ displayed the opposite alteration (Figure 3C,D). These findings are supported by protein expression in western-blotting analysis (Figure 3E,F).

3.4 | Pro-inflammatory cytokine IL1β dysregulates DNA methylation at the ABAT promoter site

According to MSP analysis, the human ABAT promoter is characterized by a typical CpG island (Figure 4A, blue highlight). To clarify the relationship between DNA methylation status and DNMT3B underexpression and ABAT overexpression, human ABAT promoter methylation was further assessed using MSP according to the recommendations of the MethPrimer software. This analysis confirmed a gradual decrease of DNA methylation at the ABAT promoter CpG site during OA progression (Figure 4B), and further suggested that inflammatory stimulation with IL1β accentuated the DNA hypomethylation in this region (Figure 4C), which likely leads to the upregulation of ABAT in ACs. In contrast, anabolic stimulation with TGFβ normalized DNA hypo-methylation at ABAT promoter site.

4 | DISCUSSION

This study describes the catabolic and anabolic state of human ACs in the early and late stages of hip FAI. Although histological findings were similar between early-FAI and late-FAI-OA, epigenetic molecule expression varied, suggesting a gradual epigenetic dysregulation during OA progression associated with FAI, confirming that early FAI is molecularly different from both advanced hip OA and healthy controls. In addition, sustained inflammatory stimulus dysregulated DNA methylation at the ABAT promoter and caused cartilage catabolism and hypertrophy for both early-FAI and late-FAI-OA.

Histological analysis revealed an OA phenotype in cartilage at the impingement zone in both early-FAI and late-FAI-OA. MMP-13 and COL10A1 elevation was observed in early-FAI and late-FAI-OA samples, confirming cartilage degeneration, catabolism, and chondrocyte hypertrophy. These findings are in agreement with previous studies,[9,10] suggesting that early OA changes already occur in the femoral head-neck cartilage area of patients with symptomatic hip FAI. Initial inflammation at the impingement zone may contribute as a

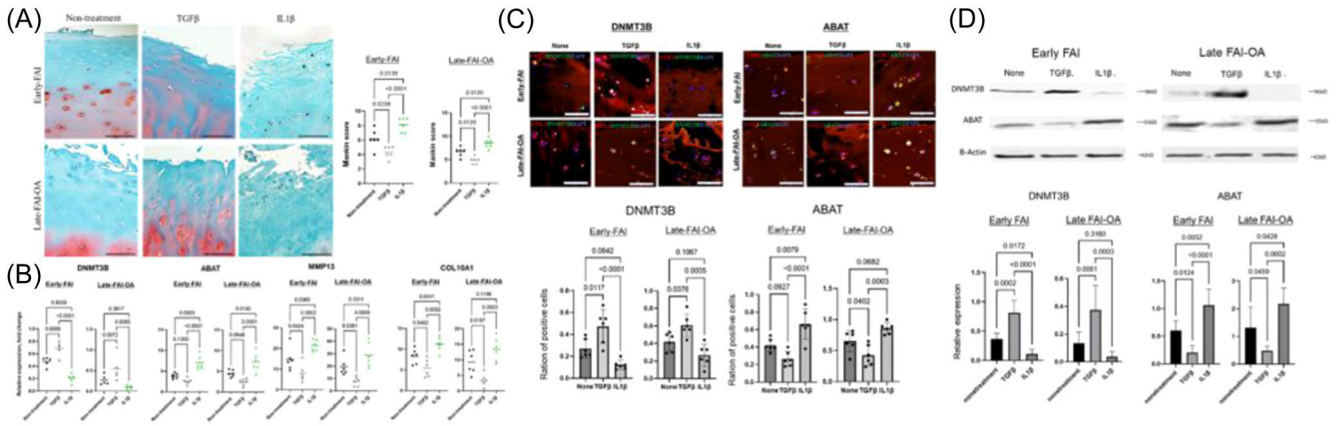

FIGURE 3 Cartilage phenotypes under catabolic and anabolic stimuli throughout disease progression. (A) Representative histologic sections with the safranin-O/fast green stain after either no treatment, anabolic stimulus with TGFβ, or catabolic stimulus with IL1β for early-FAI and late-FAI-OA samples. Scale bar: 100 μm. Graphs show quantitative comparisons of cartilage degeneration in the Mankin score system. (B) Expression of DNMT3B, ABAT, MMP13, and COL10A1 after either no treatment, anabolic stimulus with TGFβ, or catabolic stimulus with IL1β for early-FAI and late-FAI-OA samples, as determined by RT-PCR. (C) Representative immunofluorescence staining of DNMT3B (green) and ABAT (green) in cartilage sections after either no-treatment, anabolic stimulus with TGFβ, or catabolic stimulus with IL1β. COL2 (red), type II collagen; DAPI (blue) stained nuclei. Scale bar: 50 μm. (D) Bar plot showing the quantitative analysis of the ratio of positive cells. (E) Western blot analysis of DNMT3B and ABAT from cartilage samples under either anabolic stimulus with TGFβ or catabolic stimulus with IL1β for early-FAI and late-FAI-OA. βactin served as the internal control. Graphs show quantitative analysis of western blot protein levels. Early, early-FAI; FAI, femoroacetabular impingement; Late, late-FAI-OA; OA, osteoarthritis. [Color figure can be viewed at wileyonlinelibrary.com]

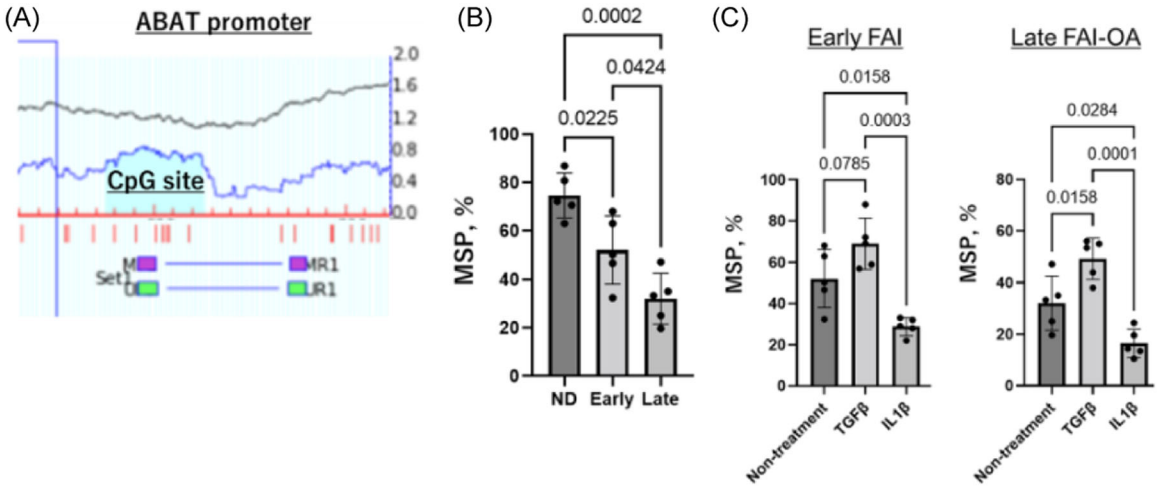

FIGURE 4 Methylation status at the ABAT promoter site. (A) Schema of human ABAT promoter. The positions of CpG (blue highlight) and MSP primer was depicted relative to the transcription starting site. (B) Quantification of MSP for the three groups. Values are normalized using input PCR and expressed as ratios of methylated/unmethylated over total PCR products. (C) Quantification of MSP for early-FAI and late-AI-OA with and without the IL1β catabolic stimulus. MSP, Methylation specific PCR; PCR, polymerase chain reaction. [Color figure can be viewed at wileyonlinelibrary.com]

molecular mechanism leading to a catabolic phenotype in chondrocytes of lateral femoral neck.[8,10] Here, we confirmed that anabolic factor TGFβ and pro-inflammatory cytokine IL1β altered the cartilage phenotype in early-FAI and late-FAI-OA samples as expected. This suggests that cartilage degeneration in the impingement zone in hip FAI is progressive at the molecular level, but could be rescued to some extent from the catabolic state, suggesting that a potential molecular therapy could beneficially alter the progression of hip FAI. Certainly, for patients with symptomatic hip cam FAI, surgical deformity correction should be prioritized to suppress molecular inflammation and improve or restore joint homeostasis. However, the high prevalence of chondral lesions in patients with FAI is well reported,[7,28–30] and the severity of cartilage damage is associated with an increased risk of poor surgical outcomes and postoperative OA progression.[29,31,32] This suggests that a molecular therapy may be useful, in the future, concomitantly to the surgical treatments, hoping to slow down OA progression during early stage of hip FAI disease. Further studies are warranted to investigate cartilage response to osteochondroplasty, removal of impingement, and/or molecular therapeutic interventions.

Importantly, this study analyzed the expression of DNMT3B and ABAT and found that in human hip ACs the expression level of DNMT3B were gradually decreased during hip OA progression while ABAT and catabolic markers were elevated. Furthermore, our MSP analysis of the ABAT promoter confirmed the DNA hypomethylation in this region as OA progresses. These findings were in line with a previous report, suggesting that the decrease in DNMT3B is associated with a significant increase in ABAT expression in human and mice OA cartilages.[14] Notably, in the current study, the inflammatory stimulus with IL1β further reduced DNA methylation at the ABAT promoter and resulted in a concomitant excessive increase of ABAT and catabolic markers in human hip OA ACs. This suggests that ABAT overexpression concomitant with DNA hypomethylation will worsen in early and late-stage FAI disease as patients continue to be exposed to additional inflammation. In contrast, anabolic stimulation with TGFβ reversed hypomethylation, suggesting an anabolic effect of TGFβ that should be investigated further as a potential future intervention. Previous in vivo studies have shown that the effect of TGFβ on cartilage depends on its concentration, with an anabolic effect with low concentrations but catabolic when using it in high dose.[33–35] Future in vivo studies are needed to explore appropriate dosage of TGFβ to induce cartilage anabolism. DNMT3B has been reported to be downregulated in OA cartilage and to play a role in mitigating extracellar matrix degradation and chondrocyte apoptosis whereby interacting with specific microRNAs.[36,37] ABAT is a key intermediate in the TCA cycle.[38] Recently, this enzyme has been reported to be increased in OA and accelerates the OA development in mice through chondrocyte hypertrophy, a catabolic phenotype, and increased mitochondria respiration.[14] Taken together with the findings from the current study, suppression of ABAT via regulation of methylation at this promoter region could deter OA progression and be a new potential target for therapeutic interventions to prevent OA progression in hip FAI.

The current study had some limitations. First, the cartilages were collected only from symptomatic patients. Inflammation may be existing at a lower level in FAI patients with minimal symptoms. Second, age and sex were not matched between early-FAI and late-FAI-OA groups. Although this would have been ideal, previous studies have reported no differences in the expression of inflammatory and catabolic molecules in cartilage samples from the head-neck junction between younger (<30 years) and older (≥30 years) patients.[39] Third, the data presented in this study did show some variability in the response to anabolic and catabolic stimulus. In the future, we will continue to analyze a larger cohort of patients to investigate better if this variability is related to severity of OA or

intraarticular inflammation. Fourth, the ideal approach should be to compare the same patients longitudinally as the disease progresses, rather than comparing patients at different stages. This would require long-term studies, but should be considered in the future. Fifth, since OA is a whole joint disease, we believe that future investigations of other key structures such as synovium will be critical to better understand the entire pathology of OA progression. However, there are ethical issues with harvesting joint tissues from early-stage patients. An animal model of OA secondary to hip FAI could provide a platform to study the mechanisms during hip OA progression in the near future.

Despite these limitations, this current study shows gradual epigenetic dysregulation of ACs during OA progression associated with FAI. Furthermore, an inflammatory stimulus altered the cartilage phenotype to a catabolic state and exacerbated aberrant epigenetic alteration in hip FAI. Future studies should involve deciphering the mechanism of how these DNMT-mediated epigenetic processes control cartilage homeostasis.

AUTHOR CONTRIBUTIONS

Tomoyuki Kamenaga: Methodology; software; formal analysis; investigation; data curation; writing – original draft preparation. **Jie Shen**: Conceptualization; methodology; writing – reviewing and editing. **May Wu**: Formal analysis; investigation; validation; data curation; writing – reviewing and editing. **Robert H. Brophy**: Data curation; writing – review and editing. **John C. Clohisy**: Data curation; writing – reviewing and editing; supervision; funding acquisition. **Regis J. O'Keefe**: Conceptualization; methodology; writing – reviewing and editing; supervision; funding acquisition. **Cecilia Pascual-Garrido**: Conceptualization; methodology, resources; date curation; writing – reviewing and editing; project administration; funding acquisition. All authors have read and approved the final submitted manuscript.

ACKNOWLEDGMENTS

The authors would like to thank Crystal Idleburg and Samantha Coleman for their technical assistance and Chadi Nahal, Gail E. Pashos, Sean M. Akers, Caroline Drain, and Karla J. Crook for their assistance. This study was supported in part by the NIH KO8 Clinical Investigator Award, 1K08AR077740-01, NIH R01 award, R01AR069605, 0REF/Goldberg Research Grant in Arthritis and the OREF Mentored Clinician Scientist Grant. Curing Hip Disease Fund and Jackie and Randy Baker Research Funds provided partial support for the research personnel.

CONFLICTS OF INTEREST

A list of author disclosures is below. O'Keefe—not related to the current work—Royalties: Fate Therapeutics; Payment for Lecture/Presentation: Visiting Professor, Loma Linda University. Clohisy—not related to the current work—Grants: Department of Defense-USAMRAA (Award # W81XWH1920042) and Zimmer Biomet; Royalties: Wolters Kluwer Health (publication) and Microport (product); Consulting: Microport Orthopedics, Inc. and Zimmer Biomet; Hip Society—Secretary and ISHA—Board member; Other financial or nonfinancial interests: CHD fund and ANCHOR. Pascual-Garrido—related to the current work—Grants: NIH and OREF/not related to the current work—Grants: Zimmer; Consulting Fees: ARVIS and Zed View Lexi 3D Developing Software. The remaining authors declare no conflict of interest.

ORCID

Robert H. Brophy http://orcid.org/0000-0002-2912-8265
Cecilia Pascual-Garrido http://orcid.org/0000-0001-7487-4753

REFERENCES

1. Kotlarz H, Gunnarsson CL, Fang H, Rizzo JA. Insurer and out-of-pocket costs of osteoarthritis in the US: evidence from national survey data. *Arthritis Rheumatol*. 2009;60:3546-3553.
2. Hootman JM, Helmick CG. Projections of US prevalence of arthritis and associated activity limitations. *Arthritis Rheumatol*. 2006;54:226-229.
3. Hsueh MF, Kraus V, Önnerfjord P. Cartilage matrix remodelling differs by disease state and joint type. *Eur Cells Mater*. 2017;34:70-82.
4. Sieker JT, Proffen BL, Waller KA, et al. Transcriptional profiling of synovium in a porcine model of early post-traumatic osteoarthritis. *J Orthop Res*. 2018;36:2128-2139.
5. Ganz R, Parvizi J, Beck M, Leunig M, Nötzli H, Siebenrock KA. Femoroacetabular impingement: a cause for osteoarthritis of the hip. *Clin Orthop Relat Res*. 2003;417:112-120.
6. Sankar WN, Nevitt M, Parvizi J, et al. Femoroacetabular impingement: defining the condition and its role in the pathophysiology of osteoarthritis. *J Am Acad Orthop Surg*. 2013;21(suppl 1):S7-S15.
7. Beck M, Kalhor M, Leunig M, Ganz R. Hip morphology influences the pattern of damage to the acetabular cartilage: femoroacetabular impingement as a cause of early osteoarthritis of the hip. *J Bone Joint Surg Br*. 2005;87:1012-1018.
8. Hashimoto S, Rai MF, Gill CS, Zhang Z, Sandell LJ, Clohisy JC. Molecular characterization of articular cartilage from young adults with femoroacetabular impingement. *J Bone Jt Surg*. 2013;95:1457-1464.
9. Haneda M, Rai MF, Cai L, et al. Distinct pattern of inflammation of articular cartilage and the synovium in early and late hip femoroacetabular impingement. *Am J Sports Med*. 2020;48:2481-2488.
10. Haneda M, Rai MF, O'Keefe RJ, Brophy RH, Clohisy JC, Pascual-Garrido C. Inflammatory response of articular cartilage to femoroacetabular impingement in the hip. *Am J Sports Med*. 2020;48:1647-1656.
11. Pascual-Garrido C, Kamenaga T, Brophy RH, et al. Otto Aufranc award: identification of key molecular players in the progression of hip osteoarthritis through transcriptomes and epigenetics. *J Arthroplasty*. 2022;37:s391-s399.
12. Reynard LN. Analysis of genetics and DNA methylation in osteoarthritis: what have we learnt about the disease? *Semin Cell Dev Biol*. 2017;62:57-66.
13. Shen J, Wang C, Li D, et al. DNA methyltransferase 3b regulates articular cartilage homeostasis by altering metabolism. *JCI Insight*. 2017;2:e9312.
14. Shen J, Wang C, Ying J, Xu T, McAlinden A, O'Keefe RJ. Inhibition of 4-aminobutyrate aminotransferase protects against injury-induced osteoarthritis in mice. *JCI Insight*. 2019;4:e128568.
15. Tonnis D, Heinecke A. Acetabular and femoral anteversion: relationship with osteoarthritis of the hip. *J Bone Joint Surg Am*. 1999;81:1747-1770.
16. Domayer SE, Ziebarth K, Chan J, Bixby S, Mamisch TC, Kim YJ. Femoroacetabular cam-type impingement: diagnostic sensitivity and specificity of radiographic views compared to radial MRI. *Eur J Radiol*. 2011;80:805-810.

17. Nepple JJ, Martell JM, Kim YJ, et al. Interobserver and intraobserver reliability of the radiographic analysis of femoroacetabular impingement and dysplasia using computer-assisted measurements. *Am J Sports Med*. 2014;42:2393-2401.
18. Yan H, Duan X, Pan H, et al. Development of a peptide-siRNA nanocomplex targeting NF- κB for efficient cartilage delivery. *Sci Rep*. 2019;9:442.
19. Pratta MA, Meo TM, Ruhl DM, Arner EC. Effect of interleukin-1-β and tumor necrosis factor-α on cartilage proteoglycan metabolismin vitro. *Agents Actions*. 1989;27:250-253.
20. McNulty AL, Rothfusz NE, Leddy HA, Guilak F. Synovial fluid concentrations and relative potency of interleukin-1 alpha and beta in cartilage and meniscus degradation. *J Orthop Res*. 2013;31:1039-1045.
21. Lafeber FP, van Roy HL, van der Kraan PM, van den Berg WB, Bijlsma JW. Transforming growth factor-beta predominantly stimulates phenotypically changed chondrocytes in osteoarthritic human cartilage. *J Rheumatol*. 1997;24:536-542.
22. Mankin HJ, Dorfman H, Lippiello L, Zarins A. Biochemical and metabolic abnormalities in articular cartilage from osteo-arthritic human hips. II. Correlation of morphology with biochemical and metabolic data. *J Bone Joint Surg*. 1971;53:523-537.
23. Livak KJ, Schmittgen TD. Analysis of relative gene expression data using real-time quantitative PCR and the 2−ΔΔCT method. *Methods*. 2001;25:402-408.
24. Zhang Q, Liu L, Lin W, et al. Rhein reverses Klotho repression via promoter demethylation and protects against kidney and bone injuries in mice with chronic kidney disease. *Kidney Int*. 2017;91:144-156.
25. Zhu X, Chen F, Lu K, Wei A, Jiang Q, Cao W. PPARγ preservation via promoter demethylation alleviates osteoarthritisin mice. *Ann Rheum Dis*. 2019;78:1420-1429.
26. Li LC, Dahiya R. MethPrimer: designing primers for methylation PCRs. *Bioinformatics*. 2002;18:1427-1431.
27. Faul F, Erdfelder E, Buchner A, Lang AG. Statistical power analyses using G*Power 3.1: tests for correlation and regression analyses. *Behav Res Methods*. 2009;41:1149-1160.
28. Pascual-Garrido C, Li DJ, Grammatopoulos G, Yanik EL, Clohisy JC. The pattern of acetabular cartilage wear is hip morphology-dependent and patient demographic-dependent. *Clin Orthop Relat Res*. 2019;477:1021-1033.
29. Domb BG, Annin S, Chen JW, et al. Optimal treatment of cam morphology may change the natural history of femoroacetabular impingement. *Am J Sports Med*. 2020;48:2887-2896.
30. Lund B, Nielsen TG, Lind M. Cartilage status in FAI patients—results from the Danish Hip Arthroscopy Registry (DHAR). *SICOT-J*. 2017;3:44.
31. Hanke MS, Steppacher SD, Anwander H, Werlen S, Siebenrock KA, Tannast M. What MRI findings predict failure 10 years after surgery for femoroacetabular impingement? *Clin Orthop Relat Res*. 2017;475:1192-1207.
32. Meier MK, Lerch TD, Steppacher SD, et al. High prevalence of hip lesions secondary to arthroscopic over- or undercorrection of femoroacetabular impingement in patients with postoperative pain. *Eur Radiol*. 2022;32:3097-3111.
33. van Beuningen HM, van der Kraan PM, Arntz OJ, van den Berg WB. Transforming growth factor-beta 1 stimulates articular chondrocyte proteoglycan synthesis and induces osteophyte formation in the murine knee joint. *Lab Invest*. 1994;71:279-290.
34. Hardingham TE, Bayliss MT, Rayan V, Noble DP. Effects of growth factors and cytokines on proteoglycan turnover in articular cartilage. *Br J Rheumatol*. 1992;31(suppl 1):1-6.
35. Bakker AC, van de Loo FAJ, van Beuningen HM, et al. Overexpression of active TGF-beta-1 in the murine knee joint: evidence for synovial-layer-dependent chondro-osteophyte formation. *Osteoarthr Cartil*. 2001;9:128-136.
36. Xiong S, Zhao Y, Xu T. DNA methyltransferase 3 beta mediates the methylation of the microRNA-34a promoter and enhances chondrocyte viability in osteoarthritis. *Bioengineered*. 2021;12:11138-11155.
37. Dou P, He Y, Yu B, Duan J. Downregulation of microRNA-29b by DNMT3B decelerates chondrocyte apoptosis and the progression of osteoarthritis via PTHLH/CDK4/RUNX2 axis. *Aging*. 2020;13:7676-7690.
38. Sarup A, Larsson O, Schousboe A. GABA transporters and GABA-transaminase as drug targets. *Curr Drug Target-CNS Neurol Disord*. 2003;2:269-277.
39. Chinzei N, Hashimoto S, Fujishiro T, et al. Inflammation and degeneration in cartilage samples from patients with femoroacetabular impingement. *J Bone Jt Surg*. 2016;98:135-141.

How to cite this article: Kamenaga T, Shen J, Wu M, et al. Epigenetic dysregulation of articular cartilage during progression of hip femoroacetabular impingement disease. *J Orthop Res*. 2023;1-9. doi:10.1002/jor.25513